Vacuum 203 (2022) 111260

Contents lists available at ScienceDirect

Vacuum

journal homepage: www.elsevier.com/locate/vacuum

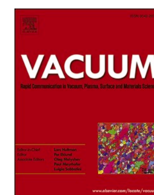

Grain boundary diffusion of Si in polycrystalline copper film

Eszter Bodnár [a], Viktor Takáts [a], Tamás Fodor [a], József Hakl [a], Yuri Kaganovskii [b], Guang Yang [c], Xiaogang Yao [d], Kálmán Vad [a,*]

[a] Institute for Nuclear Research, H-4026, Debrecen, Bem tér 18/C, Hungary
[b] Department of Physics, Bar-Ilan University, Ramat-Gan, 52900, Israel
[c] Shanghai University, School of Materials Science and Engineering, Shanghai, 200444, PR China
[d] Chinese Academy of Science, Shanghai Institute of Ceramics, Shanghai, 201899, PR China

ARTICLE INFO

Keywords:
Cu/Si nanolayers
Grain boundary diffusion
Si diffusion
Nanoscale diffusion
Low energy ion spectroscopy

ABSTRACT

Grain boundary (GB) diffusion of Si in polycrystalline Cu film was studied in the temperature range of 403–453 K, in the C-type kinetic regime. The amorphous Si layer (80 nm) and polycrystalline Cu layer (40 nm) were successively deposited by magnetron sputtering at room temperature onto a Si (111) wafer. Appearance of Si atoms on the copper surface due to GB diffusion through the copper layer was detected by low energy ion scattering spectroscopy with high sensitivity. The depth distribution of Si in Cu grain boundaries was revealed by secondary neutral mass spectrometry. Surface morphology of Cu films was investigated by scanning tunneling microscopy. Identification of Si chemical bonds on the surface layer was made by X-ray photoelectron spectroscopy. GB diffusion coefficients were estimated by the relation used for calculation of diffusant distribution from a constant source in assumption that the diffusion path equals to the film thickness at the moment of appearing Si atoms on the Cu surface. At 453 K we estimated the surface segregation factor and detected formation of Cu–O–Si atomic bonds on the Cu film surface.

1. Introduction

The modern microelectronics industry uses sub-micron size copper layers on Si wafers in order to miniaturize the electronic circuits. This raises the technical problem of reliability and requires a detailed examination of all possible processes that can occur during interaction of Cu with the Si substrate. One of these processes is the grain boundary (GB) diffusion of Si atoms through the Cu film and the subsequent accumulation on the Cu surface. This atomic migration can occur at working temperatures of electronic circuits, near room temperature, and at higher temperatures caused by heating of Cu lines by electric current. Moreover, Si atoms diffused through the Cu layer can form Cu–Si bonds on the Cu surface.

The GB diffusion coefficients D_{gb} of various elements in thin films at relatively low temperatures were successfully measured by the surface accumulation method developed by Hwang and Balluffi [1,2]. In their experiments the diffusant concentration on the surface was measured by Auger electron spectroscopy. In the present work, we report our results on low temperature diffusion of Si in copper thin films when the diffusion kinetic regime of Harrison's classification is exactly C-type [3]. However, instead of the application of the surface accumulation method [4–7], we measured the appearance time t_0 of Si atoms when Si atoms appear on Cu surface at the end of diffusion through the Cu layer. The appearance of Si atoms was detected by low energy ion scattering (LEIS), a highly surface sensitive method which is particularly applicable for this purpose [8,9]. In addition, we revealed the concentration distribution of Si atoms inside GBs of the Cu layer and estimated their surface segregation factor σ_s by mass spectrometry measurements. According to our knowledge, the surface segregation factor has not still been determined for Si in polycrystalline Cu.

2. Experiments

Samples used in our experiments were prepared by magnetron sputtering of amorphous Si layer and polycrystalline Cu layer onto (111) Si-wafer at room temperature. The thickness of the Si layer was 80 nm, while the thickness of the Cu layer was 40 nm. The vacuum in the preparation chamber was $2\cdot10^{-7}$ mbar and the working pressure during sputtering was $7\cdot10^{-3}$ mbar. High purity Ar gas was used as working gas. After preparation, the samples were transported from the preparation

* Corresponding author.
E-mail address: vad@atomki.hu (K. Vad).

https://doi.org/10.1016/j.vacuum.2022.111260
Received 25 January 2022; Received in revised form 9 June 2022; Accepted 11 June 2022
Available online 11 June 2022
0042-207X/© 2022 The Authors. Published by Elsevier Ltd. This is an open access article under the CC BY license (http://creativecommons.org/licenses/by/4.0/).

chamber into a high vacuum chamber for surface analyses achieved by X-ray photoelectron spectroscopy (XPS) and LEIS. The basic vacuum in the high vacuum chamber was near 10^{-10} mbar. XPS measurements were performed by a usual Al/Mg twin anode non-monochromatized X-ray source and a hemispherical energy analyser produced by SPECS (Berlin). In this work the Al Kα X-ray emission line (1486.6 eV) was used. The spectra were processed with the CasaXPS program.

Since a recent study has shown that adventitious carbon in a sample is an inadequate charge reference [10,11], charge referencing was performed to the $2p_{3/2}$ peak of elemental copper which was inherently present in the samples, after verifying its chemical state by Cu LMM peaks. The copper content of the samples was almost completely metallic.

In LEIS measurements 10 nA current of a He ion beam at 1 keV ion energy was applied to scan the sample surface. This He beam resulted in 10^{-7} mbar partial He pressure in the vacuum chamber. The annealing temperatures were measured by a PM100 pyrometer and were controlled by a Eurotherm temperature controller. The pyrometer was focused onto the sample holder heated by a tungsten plate. The temperature calibration was made by comparison of radiation temperature with the thermodynamic temperature measured by a thermocouple in a separate measurement.

Although 1 keV kinetic energy of the He beam is a low value, it was still high enough to cause surface etching or sputtering with the rate of 5×10^{-4} nm/s. In order to get information about the top surface layer by LEIS, which was an important requirement in our experiments, the avoidance of the weak surface etching had to be solved. So, the He ion beam was focused into a spot of 3 mm in diameter and was offset by 2 mm from the sample centre. By rotation of the sample around its centre, each LEIS measurement was performed on a new area of the sample surface. As a result of this technical solution, the etching effect during long term measurements was significantly reduced. In order to follow the possible changes in the surface morphology due to annealing and ion bombardments, and in order to determine the average grain size of the Cu film, the sample surface was checked by a scanning tunneling microscope (STM). Additionally, the depth distribution of Si in Cu-films was revealed by a secondary neutral mass spectrometer (SNMS) [12,13] right after the annealing and LEIS measurements. In SNMS, the sample surface was sputtered by an Ar ion beam through a Ta mask. The kinetic energy of Ar ions was 350 eV. The mask confined the surface sputtering to a circle shape area of 2 mm in diameter.

3. Results and discussion

GB diffusion coefficients were calculated from the time of appearance of Si atoms on the Cu surface when the silicon peak became visible in the LEIS spectrum. Since in our experiments the diffusion kinetic regime was C-type and the diffusion source was constant, we could assume that the Si distribution in copper GBs obeys the following equation [14–17].

$$C_{gb}(y) = C_0 erfc \frac{y}{2\sqrt{D_{gb}t}} \tag{1}$$

where y is the distance from the source surface, D_{gb} is the GB diffusion coefficient of Si in copper, C_0 is the concentration of diffusant atoms at the source surface, t is the diffusion time. If Si atoms reach the Cu film surface during the time t_0 (i.e. t_0 is the appearance time and $t = t_0$), the distance from the source surface is the film thickness $y = h$ and Eq. (1) can be written in the following form.

$$\frac{C_S}{\sigma_S C_0} = \frac{C_{gb}(h)}{C_0} = erfc \frac{h}{2\sqrt{D_{gb}t_0}} \tag{2}$$

Here, C_s denotes the concentration of diffusant atoms on the free copper surface (which is the accumulation surface), $C_{gb}(h)$ is the Si concentration in GBs near the free Cu surface, C_0 is the Si concentration at the interface between Cu and amorphous Si layers (this is the source surface). σ_s is the Si segregation factor in Cu. If the independent variable $\frac{h}{2\sqrt{D_{gb}t_0}}$ of the complementary error function in Eq. (2) is denoted by Z_0, i.e. $\frac{h}{2\sqrt{D_{gb}t_0}} = Z_0$, the Z_0 can be determined from Eq. (2) with the ratio of $C_{gb}(h)/C_0$ which is measured experimentally, then we obtain that

$$D_{gb} = h^2 / 4Z_0^2 t_0 \tag{3}$$

Surface morphology of the copper layer was analyzed by a high vacuum scanning tunneling microscope (STM) (Fig. 1). The size of larger grains was around 40 nm in accordance with the film thickness. The Si concentration on the Cu layer, or Si coverage of the sample surface, was measured by LEIS. Fig. 2 shows some LEIS spectra measured on a sample surface which was annealed at 403 K. The spectra show the intensity changes of the scattered He ions at three different energies according to Si, Cu and O masses. The Si peak increases with the increase in annealing time, while the Cu and O peaks decrease due to surface coverage by Si. The oxygen is important from the point of view of surface impurity. It could derive from the residual gas of the preparation chamber and from the sample transportation. During sample transport from the preparation chamber to the high vacuum LEIS/XPS chamber, the sample surface was exposed to air. Although surface cleaning was applied prior annealing, a small oxygen contamination is still reflected in the LEIS spectra. Oxygen can modify the properties of a nanolayer, e.g. the electrical properties or surface morphology [18], but in our case there is no reason to modify the atomic motion mechanism. The oxygen concentration on the surface was too small and the temperature was too low to bring about any volume segregation. There is also no surface segregation as the LEIS measurements show in Fig. 2.

The inset of Fig. 2 shows that the Si peak increased with annealing time according to the increase in Si content of the surface layer. The peak area is proportional to Si content of the surface layer. This proportionality allowed us to determine the appearance time of Si with a sufficient accuracy by approximation of this area to zero. The nanoscale GB diffusion coefficient can be determined by the appearance time measurement using Eq. (3). This solution made it possible for us to study the GB diffusion at rather low temperatures where the diffusion mechanism is purely C-type.

Typical depth distributions of Si and Cu in the Cu/Si bilayer system before and after sample annealing are demonstrated in Fig. 3. The depth distributions were revealed by SNMS. The sample was annealed at 453 K for 5 min. The Si intensity, which is proportional to Si concentration in grain boundaries, depends on the depth and drops gradually from $C_0 = 6 \cdot 10^3$ cps to $C_{gb}(h) = 570$ cps and increases again on the Cu layer surface due to surface segregation and surface accumulation. From $C_{gb}(h)$ and the concentration of diffusant atoms on the accumulation surface ($C_S = 2900$ cps), the segregation factor can be calculated, $\sigma_s = C_S/C_{gb}(h)$. We received that the segregation factor of Si in Cu at 453 K is $\sigma_s = 5.1$. The Si depth distribution in GBs defines the ratio of $C_{gb}(h)/C_0$. It is about 0.095 which according to Eq. (2) corresponds to erfc(Z_0) with $Z_0 = 1.118$. Inserting this value into Eq. (3), the GB diffusion coefficient can be calculated in the form of $D_{gb} = h^2/(5 \cdot t_0)$.

The GBs were filled up by Si during the appearance time. The average distribution along GBs immediately after filling is shown in Fig. 3 by the section of the line between the points of C_0 and $C_{gb}(h)$. This distribution remained unchanged for the rest of the annealing time. In C-type kinetic diffusion regime, Si atoms are only located inside GBs, but there is no information about the local concentration inside GBs. By depth profiling we can only measure the average concentration distribution. Near the sample surfaces the Si concentration is about 1 at%. We can also determine the GB width and dimensionality of diffusional space. The mean squared displacement of a Si atom inside a GB, due to diffusion, is described by the Einstein-Smoluchowski relation, $< r^2(t) > = (2d) \cdot D_{gb} t$, where $r(t)$ is the displacement, t is the time, D_{gb} is the GB diffusion coefficient, and d is the dimension of the space where the atomic motion

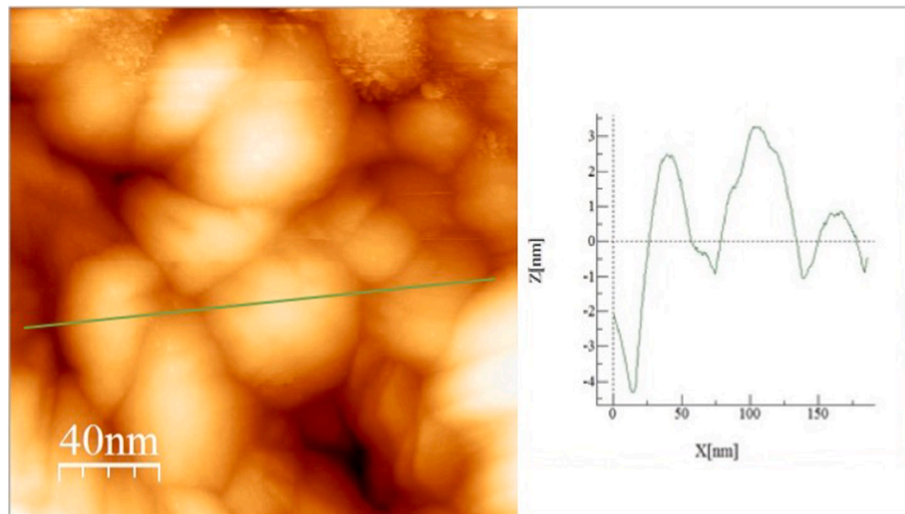

Fig. 1. Typical STM picture of a 40 nm thick Cu films immediately after deposition.

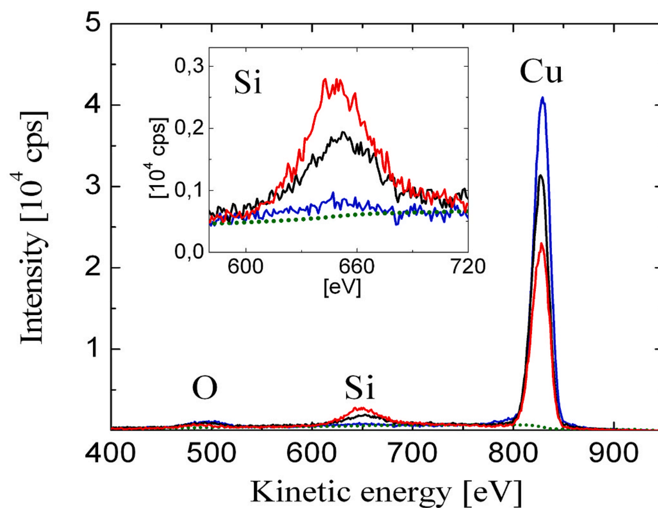

Fig. 2. LEIS spectra of O, Si and Cu elements at 403 K, after 10 min (blue line), 32 min (black line) and 57 min (red line) annealing. The dotted line is the background.

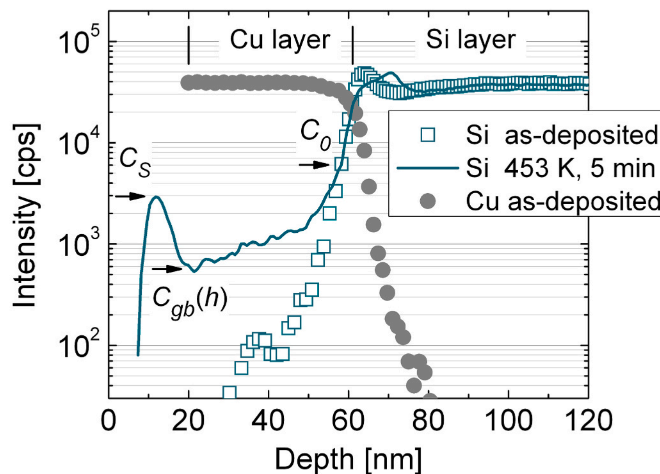

Fig. 3. Depth distributions of Si obtained by SNMS before (symbols) and after GB diffusion (line).

takes place [see e.g. Ref. [19]]. The constant 2*d* on the right side of this equation equals to 2 if the atomic motion (or the diffusion type) is one dimensional (1D), to 4 for two-dimensional (2D) diffusion, and to 6 for three-dimensional (3D) diffusion. In the previous paragraph, we obtained 5 for this constant. This can be interpreted as the type of diffusion being between 2D and 3D. The experimentally measured GB widths in different metallic systems were collected by Prokoshkina et al. [20]. The authors found that the GB width is in the range of 0.2–3 nm. If the GB is narrow, a few Å, the diffusion takes places in 2D space. If the GB width is large, a few nm, the diffusion space is 3 dimensional. Since in our measurements the diffusion type is between 2D and 3D, the GB width may be large, even 1 nm. From the average Si concentration measured experimentally near the surface (1 at%), from the GB width, and from the total length of GBs we can make an estimation for the density of Si in GBs. Fig. 1 shows that the total volume of GBs is much higher than 1% of the sample volume. We can thus suppose that GBs contain the 1 at% Si in low density form. Si concentration depends on the depth and it increases with the approach of the source surface (Fig. 3). The question arises whether the same concentration dependence is valid for D_{gb}, but these experiments cannot answer this question.

Temperature dependence of the diffusion coefficient is Arrhenius-type, so D_{gb} can be written in the form of $D_{gb} = D_{gb0} \bullet exp(-\Delta H_{gb}/RT)$, where D_{gb0} is a pre-exponential factor, ΔH_{gb} is the activation enthalpy of GB diffusion, R and T are the gas constant and temperature. Plotting the experimentally measured D_{gb} values in a lnD_{gb} vs. $1/T$ coordinate system, the slope of linear fit yields the activation enthalpy (Fig. 4). For the activation enthalpy, we obtained $\Delta H_{gb} = (98 \pm 7)$ kJ/mol = (1.02 ± 0.07) eV/atom. The intersection of lnD_{gb} axis yields the pre-exponential factor $D_{gb0} = (6.0 \pm 0.9) \cdot 10^{-6}$ m^2/s.

As we mentioned previously, Si peak area is proportional to the surface area covered by Si. Time evolution of this peak area reflects the progress of Si surface coverage in time. Fig. 5 shows this progress in the temperature range of 403–453 K. It can be seen that the surface Si content grew in time and reached a saturation near 28% coverage. The saturation corresponds to the maximum surface coverage which can be achieved by thermally induced surface accumulation in C-type kinetic diffusion regime. As it can be seen in Fig. 5, the surface coverage increases rapidly just after the appearance time, due to high atomic flux through GBs. However, when Si coverage approaches its saturation value, the atomic flux decreases. Finally, the diffusion stops. The reason for stopping is that the Si concentration at the source surface (which is the Cu/Si interface) is significantly decreased and the constant nature of the source surface disappears. The empty space of the Si layer at the interface is filled with Cu atoms resulting in mixing of Cu and Si atoms.

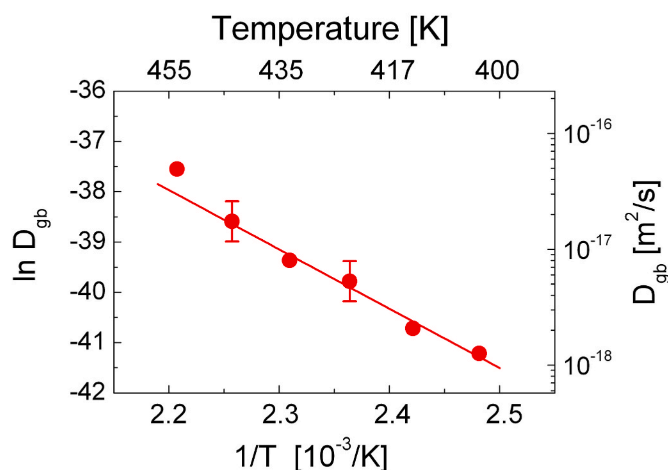

Fig. 4. Temperature dependence of Si grain boundary diffusion coefficient in Cu nanocrystalline layer. The measurements were carried out in the temperature range of C-type diffusion kinetic regime. The highest temperature 453 K seems to be at the border between the C- and B-type kinetic regimes, so the linear curve was not fitted to this data.

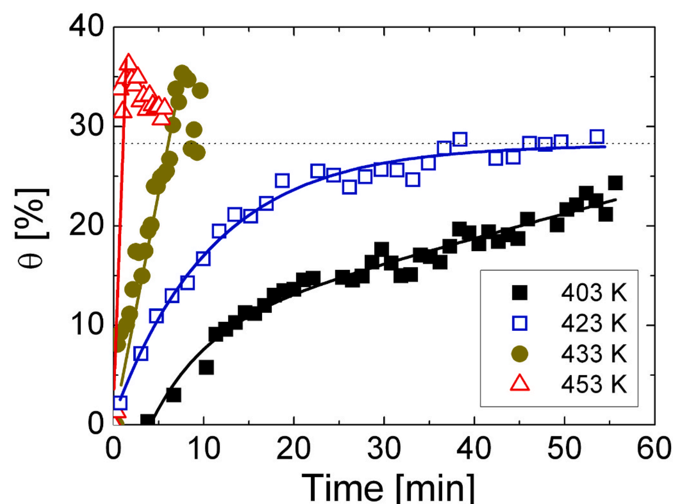

Fig. 5. Time dependence of Si content of the Cu film surface at various temperatures. Θ is the surface coverage.

According our measurements, about 80% of Si atoms is replaced by Cu atoms before the diffusion stops.

After the highest annealing temperature which was applied in these experiments (453 K), the chemical bonds of surface Cu atoms were identified by XPS. We measured the energy spectrum of photoelectrons (Fig. 6) and analyzed its structure by CasaXPS software. It was found that the binding energy of Cu $2p_{3/2}$ electrons shows an additional peak besides the Cu–Cu bonds (red line) which corresponds to Cu–O–Si bonds (blue line). The binding energy shift towards higher energy suggests a $CuSiO_3$-like phase formation of Si on the Cu surface and with surface oxygen. The ratio of Cu–O–Si bonds among all copper bonds was about 0.06 while the Si coverage of the surface was near 30%.

The aim of this XPS analysis was to find the answer to the question whether the silicon forms a chemical compound with the copper layer or not. If Cu is deposited on a Si layer, Cu_3Si compound is formed already at 453 K temperature [21,22]. However, if the interface is prepared in opposite direction, i.e. the Cu layer is covered by Si, the question is whether the Cu_3Si compound is also formed or not. It was found that this phase could not be detected by our experimental arrangement, as Fig. 6 shows.

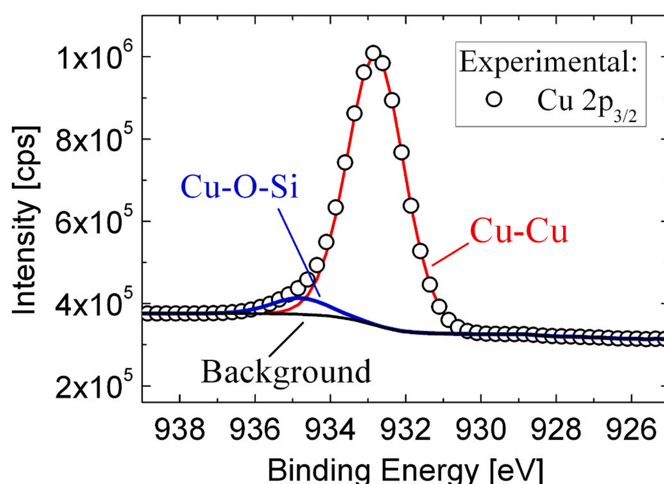

Fig. 6. Binding energy of Cu $2p_{3/2}$ electrons after the sample was annealed at 453 K for 10 min. The circles denote the experimental values, while the red and blue lines are the results of peak deconvolution made by CasaXPS software. The peak structure shows that 94.3% of the whole Cu bonds are Cu–Cu bonds and 5.7% are Cu–O–Si bonds.

4. Conclusions

Grain boundary diffusion of Si atoms into polycrystalline thin Cu film having the thickness of $h = 40$ nm was studied by low energy ion scattering, secondary neutral mass spectroscopy and X-ray photoelectron spectroscopy. LEIS allowed us to estimate the diffusion time (t_0) of Si through the GBs of Cu film, as well as the accumulation kinetics of Si on the Cu surface. In the temperature range of 403–453 K, in pure C-type diffusion kinetic regime, the GB diffusion coefficient was estimated from the equation $D_{GB} = h^2/(5 \cdot t_0)$ and found the formula of $D_{GB} = (6.0 \pm 0.9) \cdot 10^{-6} \cdot \exp(-(98 \pm 7)\ kJ/mol/RT)$. From the Si concentration on the Cu surface at saturation state and from the Si distribution along copper GBs, the surface segregation factor of Si could be determined. At 453 K, we received for Si segregation in Cu that $\sigma_s = 5.1$. At the end of segregation process, Cu–O–Si bonds could be detected by XPS reflecting that the adjacent Si and Cu atoms on the surface form chemical bonds with surface oxygen atoms.

CRediT authorship contribution statement

Eszter Bodnár: Software, Methodology, Investigation, Data curation. **Viktor Takáts:** Supervision, Investigation, Data curation, Conceptualization. **Tamás Fodor:** Investigation, Data curation. **József Hakl:** Validation, Formal analysis. **Yuri Kaganovskii:** Writing – original draft, Validation, Conceptualization. **Guang Yang:** Investigation, Data curation. **Xiaogang Yao:** Investigation, Data curation. **Kálmán Vad:** Writing – original draft, Supervision, Investigation, Conceptualization.

Declaration of competing interest

The authors declare that they have no known competing financial interests or personal relationships that could have appeared to influence the work reported in this paper.

Data availability

No data was used for the research described in the article.

Acknowledgement

This work was supported by the projects TKP2021-NKTA-42 and 2019-2.1.7-ERANET-2021-00021 financed by the National Research,

Development and Innovation Fund of the Ministry for Innovation and Technology, Hungary.

References

[1] J.C.M. Hwang, R.W. Balluffi, Measurement of grain boundary diffusion at low temperatures by the surface accumulation method. I. Method and analysis, J. Appl. Phys. 50 (1979) 1339–1348, https://doi.org/10.1063/1.326168.

[2] J.C.M. Hwang, J.D. Pan, R.W. Balluffi, Measurement of grain boundary diffusion at low temperature by the surface accumulation method. II. Results for goldsilver system, J. Appl. Phys. 50 (1979) 1349–1359, https://doi.org/10.1063/1.326115.

[3] L.G. Harrison, Influence of dislocations on diffusion kinetics in solids with particular reference to the alkali halides, Trans. Faraday Soc. 57 (1961) 1191–1199, https://doi.org/10.1039/TF9615701191.

[4] Z. Bastl, J. Zidu, K. Rohacek, Determination of the diffusion coefficient of aluminium along the grain boundaries of gold films by the surface accumulation method, Thin Solid Films 213 (1992) 103–108.

[5] Z. Erdélyi, Ch Girardeaux, G. Langer, L. Daróczi, A. Rolland, D. Beke, Determination of grain boundary diffusion coefficients by Auger electron spectroscopy, Appl. Surf. Sci. 162–163 (2000) 213–218.

[6] G. Erdelyi, G. Langer, J. Nyeki, L. Kover, C. Tomastik, W.S.M. Werner, A. Csik, H. Stoeri, D.L. Beke, Investigation of Ta grain boundary diffusion in copper by means of Auger electron spectroscopy, Thin Solid Films 459 (2004) 303–307, https://doi.org/10.1016/j.tsf.2003.12.125.

[7] Z. Balogh, Z. Erdélyi, D.L. Beke, A. Portavoce, Ch. Girardeaux, J. Bernardini, A. Rolland, Determination of grain boundary diffusion coefficients in C-regime by Hwang-Balluffi method: silver diffusion in Pd, Defect Diffusion Forum 289–292 (2009) 763–767. http://www.scientific.net/DDF.289-292.763.

[8] H.H. Brongersma, M. Draxler, M. de Ridder, P. Bauer, Surface composition analysis by low-energy ion scattering, Surf. Sci. Rep. 62 (2007) 63–109, https://doi.org/10.1016/j.surfrep.2006.12.002.

[9] L.V. Takáts, A. Csik, J. Hakl, K. Vad, Diffusion induced atomic islands on the surface of Ni/Cu nanolayers, Appl. Surf. Sci. 440 (2018) 275–281, https://doi.org/10.1016/j.apsusc.2018.01.087.

[10] G. Greczynski, L. Hultman, Compromising science by ignorant instrument calibration - need to revisit half a century of published XPS data, Angew. Chem. Int. Ed., 10.1002/anie.201916000.

[11] G. Johansson, J. Hedman, A. Berndtsson, M. Klasson, R. Nilsson, Calibration of electron spectra, J. Electron. Spectrosc. Relat. Phenom. 2 (1973) 295–317.

[12] H. Oechsner, L. Reichert, Energies of neutral sputtered particles, Phys. Lett. 23 (1966) 90–92.

[13] K. Vad, A. Csik, G.A. Langer, Secondary neutral mass spectrometry – a powerful technique for quantitative elemental and depth profiling analyses of nanostructures, Spectrosc. Eur. 21 (2009) 13–16.

[14] J. Crank, The Mathematics of Diffusion, Clarendon Press, Oxford, 1975, p. 21.

[15] Y. Mishin, Chr Herzig, J. Bernardini, W. Gust, Grain boundary diffusion: fundamentals to recent developments, Int. Mater. Rev. 42 (1997) 155–178.

[16] C. Herzig, Y. Mishin, in: P. Heitjans, J. Kärger (Eds.), Grain Boundary Diffusion in Metals, Diffusion in Condensed Matter, Springer Verlag, Berlin, 2005, p. 350.

[17] A. Paul, T. Laurila, V. Vourinen, S.V. Divinski, Thermodynamics, Diffusion and the Kirkendall Effect in Solids, Springer International Publishing, Switzerland, 2014, p. 446.

[18] L. Wang, Y. Zhong, J. Li, W. Cao, Q. Zhong, X. Wang, X. Li, Effect of residual gas on structural, electrical and mechanical properties of niobium films deposited by magnetron sputtering deposition, Mater. Res. Express 5 (2018), 046410, https://doi.org/10.1088/2053-1591/aab8c1.

[19] J. Philibert, One and a half century of diffusion: Fick, Einstein, before and beyond, Diffus. Fundam. 4 (2006) 6.1–6.19.

[20] D. Prokoshkina, V.A. Esin, G. Wilde, S.V. Divinski, Grain boundary width, energy and self-diffusion in nickel: effect of material purity, Acta Mater. 61 (2013) 5188–5197.

[21] R.R. Chromik, W.K. Neils, E.J. Cotts, Thermodynamic and kinetic study of solid state reactions in the Cu–Si system, J. Appl. Phys. 86 (1999) 4273–4281, https://doi.org/10.1063/1.371357.

[22] B. Parditka, M. Verezhak, Z. Balogh, A. Csik, G.A. Langer, D.L. Beke, M. Ibrahim, G. Schmitz, Z. Erdélyi, Phase growth in an amorphous Si–Cu system, as shown by a combination of SNMS, XPS, XRD and APT techniques, Acta Mater. 61 (2013) 7173–7179, https://doi.org/10.1016/j.actamat.2013.08.021.